Force of an Actin Spring

Jennifer H. Shin,*†‡ Barney K. Tam,†§ Ricardo R. Brau,¶ Matthew J. Lang,*¶ L. Mahadevan,‡‖ and Paul Matsudaira†¶**

*Department of Mechanical Engineering, §Department of Physics, ¶Division of Biological Engineering, **Department of Biology, Massachusetts Institute of Technology, Cambridge, Massachusetts; †Whitehead Institute for Biomedical Research, Cambridge, Massachusetts; ‡Division of Engineering and Applied Sciences, and Department of Organismic and Evolutionary Biology, Harvard University, Cambridge, Massachusetts; and ‖Department of Systems Biology, Harvard Medical School, Boston, Massachusetts

ABSTRACT Cellular movements are produced by forces. Typically, cytoskeletal proteins such as microtubules and actin filaments generate forces via polymerization or in conjunction with molecular motors. However, the fertilization of a *Limulus polyphemus* egg involves a third type of actin-based cellular engine—a biological spring. During the acrosome reaction, a 60-μm long coiled and twisted bundle of actin filaments straightens and extends from a sperm cell, penetrating the vitelline layer surrounding the egg. A subtle overtwist of 0.2°/subunit underlies the mechanochemical basis for the extension of this actin spring. Upon calcium activation, this conformational strain energy is converted to mechanical work, generating the force required to extend the bundle through the vitelline layer. In this article, we stall the extension of the acrosome bundle in agarose gels of different concentrations. From the stall forces, we estimate a maximum force of 2 nN and a puncturing pressure of 1.6 MPa. We show the maximum force of extension is three times larger than the force required to puncture the vitelline layer. Thus, the elastic strain energy stored in the acrosome bundle is more than sufficient to power the acrosome reaction through the egg envelope.

INTRODUCTION

Cellular engines at the molecular level typically generate picoNewton levels of force and nanometer-scale movements. For example, a molecular motor such as myosin produces ~3 pN of force from an ATP-coupled conformational change in the head and neck domains to step along an actin filament in nanometer increments (1–4). Polymers such as actin and tubulin generate pN forces as a subunit adds to the end of a filament or tubule (5). Assembly into macromolecular complexes multiplies the forces generated by each protein. The μN of force generated by a muscle myofibril is the product of individual myosin molecules arranged in parallel and in series with a lattice of actin filaments (6). Protrusion of the cell membrane results from extension at the free ends of a network of branched and cross-linked actin filaments (7). Thus, typical cellular engines integrate motors or single filament polymerization into a larger structure to generate nanoNewton-scale forces required for micrometer-scale cellular movements (8).

The acrosome reaction in sperm cells of horseshoe crab *Limulus polyphemus* provides a spectacular example of nontraditional actin motility. To initiate fertilization, *Limulus* sperm cells must penetrate two layers surrounding the egg, an outer basement lamella ~5-μm thick and an inner vitelline envelope ~35-μm thick. Sperm cells penetrate this physical barrier by uncoiling and extending a 60-μm long bundle of actin (9) (Fig. 1 *A*). Structural analysis reveals that, before reacting, the acrosome bundle consists of a paracrystalline array of bent, twisted actin filaments bound to two proteins—scruin and calmodulin. This bundle is wrapped around the base of the nucleus in a helical coil (10). In the presence of Ca^{2+}, scruin changes conformation (11), causing the individual actin filaments to untwist and extend to a homogeneous, straightened bundle called the true discharge (TD) (10). This motility does not involve ATP hydrolysis or a myosin motor protein (10,12). Using electron micrographs of the actin bundle before and after activation, DeRosier and Tilney suggested that the force underlying this motility is a spring-based mechanism in which mechanical energy is stored in slight but concerted overtwists of the actin filaments in the bundle, and our quantitative experiments confirm this hypothesis (13–15). Thus the *Limulus* sperm acrosome bundle is an example of a third type of actin-based cellular engine—a mechanochemical spring where the relevant displacement governing force generation arises from an overtwist rather than from a rectilinear extension or compression from equilibrium.

In this work, we measure and report the maximum force generated by the *Limulus* acrosome reaction. First, we embed sperm cells in a solid block of agarose and trigger the cells to extend the acrosome bundle through a solid block of agarose. During the extension, the acrosome bundle moves against a shear drag exerted by the agarose, and the reaction stalls when the opposing force exceeds the force produced by the acrosome reaction. The stall force is calculated from measurements of the stalled bundle lengths at various agarose concentrations together with stress values from penetration tests of agarose. To corroborate our measurements, we also use methylcellulose (MC) as a viscoelastic thickening agent to mechanically slow

Submitted November 8, 2006, and accepted for publication February 1, 2007.

Address reprint requests to Paul Matsudaira, E-mail: matsudaira@wi.mit.edu.

Jennifer H. Shin's present address is Dept. of Mechanical Engineering, Korea Advanced Institute of Science and Technology, Science Town, Daejeon, 305-701, Republic of Korea.

0006-3495/07/05/3729/05 $2.00

doi: 10.1529/biophysj.106.099994

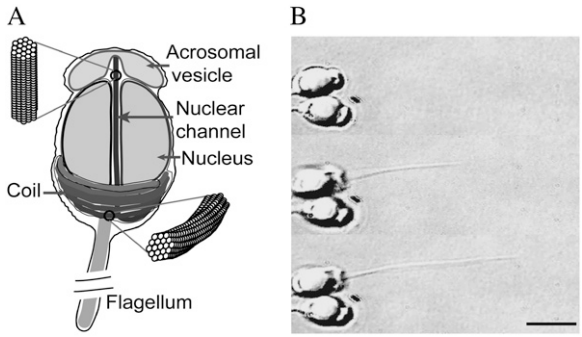

FIGURE 1 The acrosome reaction in *Limulus* sperm. (*A*) A schematic of an unreacted sperm cell inspired from electron micrographs, showing the proximal end of the acrosome bundle lying in the nuclear channel while the rest of the bundle is coiled around the base of nucleus. (*Insets*) The filaments are twisted in the coiled state, but parallel to each other in the true-discharge (TD) state. (*B*) Upon laser activation, a sperm cell embedded in agarose extends the acrosome bundle to a final length of ~15 μm; normally, the cell extends the bundle to a length of 50–60 μm in artificial sea water (scale bar = 5 μm).

down the extension rate of the acrosome bundle. This method yields a lower bound estimate of the acrosome reaction force, providing an independent verification of our measured stall force. Our work provides the first estimate of the force associated with the mechanochemical conformation change in a bundle of actin.

MATERIALS AND METHODS

Reaction medium

For the agarose experiments, 0.5% (w/v), 1.0%, 1.5%, 2%, 2.5%, and 3% agarose gels are prepared by mixing low-melting-point agarose powder (gel point: 29°C) in artificial seawater (ASW: 423 mM NaCl, 9 mM KCl, 9.27 mM $CaCl_2$, 22.94 mM $MgCl_2$, 25.5 mM $MgSO_4$, 2.15 mM $NaHCO_3$, 10 mM Tris, pH-adjusted to 7.9–8.0). The mixture of agarose powder and ASW is heated to ~80°C with gentle stirring using a magnetic stir bar until the agarose is completely dissolved. The solution is left to solidify at room temperature (25°C) until the cooled agarose gel becomes translucent. Since the agarose solution exhibits a hysteresis between its melting point (>50°C) and gel point (29°C), the prepared agarose block is remelted at 65–70°C for 10 min and stored in aliquots at 4°C for acrosome reaction experiments and characterization experiments.

Embedding sperm cells in agarose

Horseshoe crab (*Limulus polyphemus*) sperm (500 μl) is collected from a healthy male and stored on ice. The collected sperm are washed at least twice in ASW by centrifugation at 750 × *g* for 5 min. Washed sperm cells are diluted 1:2000 in ASW, injected into a flow chamber that is pretreated with a tissue adhesive, BIOBOND (Cat. No. 71304, EMS, Fort Washington, PA), and incubated for 10–20 min for cells to securely adhere to the bottom of the flow chamber. The sperm-containing flow cell is warmed to ~30°C on a heating block and the precooled molten agarose (32°C) is injected into the chamber, completely replacing the ASW. The agarose-filled flow chamber is rapidly cooled to 4°C. Analyses by electron microscopy indicated that the rapidly cooled gels have a homogeneous pore structure (16). The low-melting-point agarose is ideally suited for our experiments as sperm cells are viable up to ~40°C.

Inducing the acrosome reaction

All microscopy work was performed on a Nikon TE2000 inverted microscope with DIC optics and an oil immersion objective (Nikon, Melville, NY). Images were captured with a Sony S-VHS video recorder (Sony, Tokyo, Japan) and digitized to a PC for analysis. Typically, the acrosome reaction in the *Limulus* sperm, as well as in other marine invertebrate sperm, is triggered by flowing calcium ionophore, which transports extracellular Ca^{2+} into the cytoplasm. Our recent finding has shown that a focused 488-nm laser can also induce the acrosome reaction when it is used to irradiate certain regions of the sperm cell. For efficient triggering, we focus the beam to a diffraction-limited spot using a 100 × 1.4 N.A. microscope objective lens. Measured immediately before entering the objective lens, the beam intensity is ~7 mW. Compared to the traditional use of calcium ionophore for activation, our newly discovered laser irradiation allows us to trigger the acrosome reaction on selected cells on demand, and even on cells embedded in solid media.

Characterizing agarose

We perform penetration tests with a Materials Testing Machine (Zwick TC-FR010TH Allround-Line; Kennesaw, GA) to characterize the shear and crack opening stresses agarose exerts on the extending acrosome bundle. We operate the instrument in a compression mode, moving the probe at a fixed velocity. The probe is mounted on a load cell (Zwick KAP-TC 10N), a device which converts mechanical force into an electrical signal. This load cell monitors the amount of force exerted during compression to maintain a fixed velocity as the probe is moved through the agarose block.

In this study, we assume that the agarose is a homogeneous continuous medium. For such an ideal solid, the shear stress along the probe is independent of the probe diameter and thus the frictional force that resists the motion of the probe simply scales with the diameter of the probe. Furthermore, the stress is not a function of the traveling velocity of the probe. To a first approximation, it is reasonable also to assume that surface interaction of agarose with a metal probe is similar to that of the actin bundle and agarose, for both the metal probe and bundle are crystalline structures.

We choose a stainless steel probe of $R_{\mathrm{rod}} = 0.54$ mm with a tapering tip, and set the probe velocity to 1.0 mm/s so that the normalized velocity $\tilde{V} = V/R_{\mathrm{Rod}} \sim 2\mathrm{s}^{-1}$, corresponds to the acrosome reaction velocity of 0.1 μm/s for the bundle of 50-nm tip diameter. As shown in Fig. 2 *B*, the probe is set to penetrate and puncture through an agarose block of thickness δ. We measured the distance traveled by the rod through the agarose as a varying force is applied to maintain a preset velocity. The force-displacement curve consists of distinct transient (I) and steady-state (II) regimes as shown in Fig. 2 *C*. While penetrating through the block, the force exerted by the load cell is opposed by two forces, namely the crack opening force associated with the development of a crack in front of the extending tip, F_{crack}, and the frictional shear force along the surface of the probe, F_{drag}. We treat these two forces as additive so that $F_{\mathrm{total}} = F_{\mathrm{crack}} + F_{\mathrm{drag}}$. Once the rod punctures through the slab, it reaches a steady state where only the frictional force opposes the motion, since there is no longer agarose in front of the tip. From the steady-state force, F_{ss}, we calculate the steady-state shear stress from the frictional drag along the bundle, $\tau = F_{\mathrm{ss}}/2\pi R_{\mathrm{rod}}\delta$, where δ is the total thickness of the agarose block. The crack opening force is then calculated by subtracting the frictional drag force from the total force, $F_1, F_2, F_3, \ldots, F_{\mathrm{n}}$, in the transient regime (I) as in $F_{\mathrm{crack}} = F_{\mathrm{n}} - F_{\mathrm{ss}} = F_{\mathrm{n}} - \tau 2\pi R_{\mathrm{rod}}(d_{\mathrm{n}} - d_0)$. We repeat the experiments while varying the diameter of the probes and the penetration velocities to verify that the effects of these parameters in the stress measurements are not significant.

Characterizing methyl cellulose

We use MC solution to mechanically slow down the acrosome reaction. To determine the viscosity of MC solution, we apply a Stokes' drag force to a laser-trapped 0.5-μm diameter glass bead in MC solutions. This method

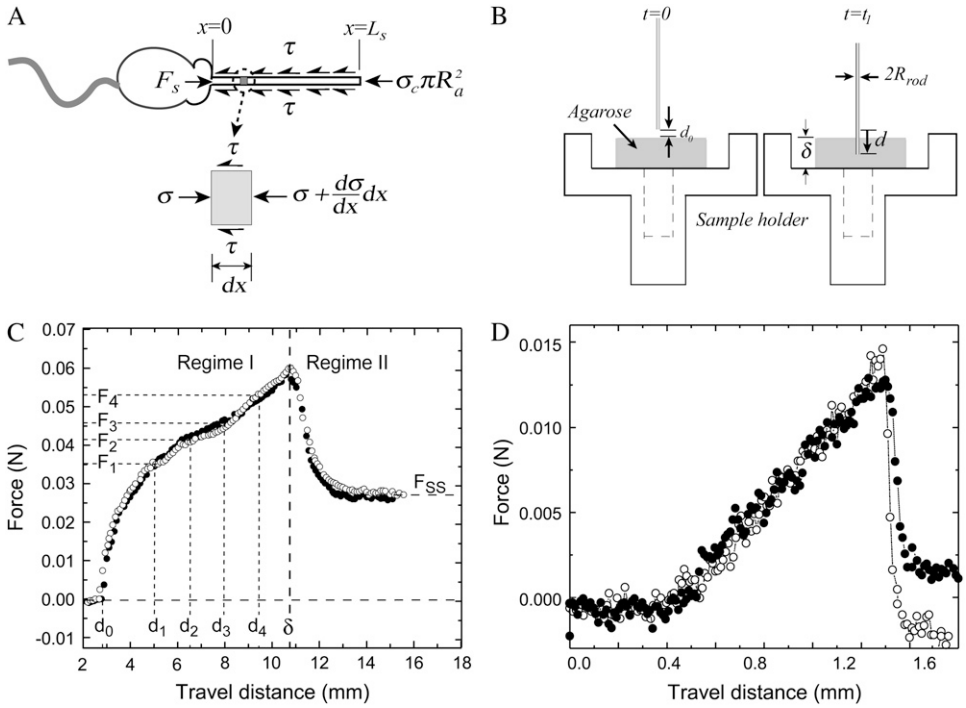

FIGURE 2 Analysis to determine forces opposing acrosome bundle extension. (*A*) Forces acting on the extending acrosome bundle. When the embedded cells react, the extending acrosome bundle inside the agarose is opposed by both a frictional force, F_{drag}, along the bundle and a crack opening force F_{crack} at the tip. We balance forces on a differential element of the bundle at the moment it stalls, $x = L_s$, to estimate F_s. (*B*) A specimen holder has a through-hole in the middle so that the probe can puncture through the slab of agarose gel. (*C*) Force versus travel distance of the probe ($R_{\text{rod}} = 0.54$ mm) as it penetrates through a slab of 3% agarose. The probe makes initial contact with the gel when $d = d_0$ and penetrates through when $d = \delta$. In the transient region I, both frictional drag and crack opening force oppose the penetrating probe while only frictional drag exists in the steady-state regime II. (*D*) Force versus travel distance from the puncture test on *Limulus* eggs using 100-μm radius platinum wire.

probes a length-scale comparable to that of the bundle diameter, a factor not shared by more conventional rheology methods. We trap the bead with the laser trap, then move the stage, and thus MC solution, at a controlled velocity. The moving fluid induces a drag force on the bead and displaces it from the center of the trap. The trap behaves like a spring, exerting a linear restoring force $F_{\text{trap}} = -kx$ on the bead. The distance, x, is measured from the center of the trap, and the spring constant, k, is found via the equipartition theorem $(1/2)k\langle x^2\rangle = (1/2)k_{\text{B}}T$ with one degree of freedom. By balancing Stokes' drag with the linear restoring force of the trap, we find the viscosity of the solution.

RESULTS AND DISCUSSION

When activated in ASW, a 60-μm long actin bundle extends from the cell in 15 s. However, in agarose, the bundle extends at a much slower rate and stalls before full extension. This occurs because the bundle is opposed by two forces. While tunneling through the block, the total force opposing the bundle motion is the sum of two linear forces—a macroscopic-shear stress and a crack-opening stress. As a result of this total force, the acrosome extension in agarose is stalled at a shortened length.

To quantify the force exerted during the TD reaction, we balance the forces in the acrosome bundle-agarose system (Fig. 2 *A*). Because a 1.5% agarose block has an average pore size of 150 nm and higher concentrations only reduce the pore sizes (17), we treat agarose as a homogenous continuous solid. Doing so on the bundle at the moment it stalls $x = L_{\text{s}}$ yields an expression for the acrosome stalling force F_{s}:

$$F_{\text{s}} = F_{\text{crack}} + F_{\text{drag}} = \sigma_{\text{c}}\pi R_{\text{a}}^2 + \tau 2\pi R_{\text{a}} L_{\text{s}}. \qquad (1)$$

Here R_{a} is the acrosome bundle radius, the first term is the force required to open a crack and the second is the frictional force associated with moving the bundle relative to the agarose, where τ is the shear stress, and σ_{c} the crack opening stress associated with the penetration of the agar by the actin bundle. To determine the shear stress, τ, and crack-opening stress, σ_{c}, we carry out penetration tests on agarose using needles of various diameters. The shear stress, τ, measured at steady state exhibits gradual increase with agarose concentration. The crack-opening stress, σ_{c}, shows a minor increase from 2% (w/v) to 2.5% agarose, but it almost doubles from 2% to 3% agarose. Because both crack opening and shear stresses increase at higher concentrations of agarose (Fig. 3 *C*), the stall length of the acrosome bundle shortens (Fig. 3 *B*). Fig. 3 *C* shows the magnitudes of the shearing-drag stress and crack-opening stress measured with a stainless steel probe of $R_{\text{rod}} = 0.54$ mm at a probe velocity of 1.0 mm/s. The dominant component of the total force is frictional drag, since the crack-opening force contributes $<10\%$ to the total. Using estimates of the shear stress τ, the crack-opening stress σ_{c}, and the stall lengths L_{s} at various agarose concentrations, we obtain the acrosome reaction force at the moment of stalling using Eq. 1 (Fig. 3 *D*). Averaging the results from our calculations, we arrive at an acrosome stalling force of $F_{\text{s}} \sim 1.9$ nN (Fig. 3 *D*).

We also consider the shear-stress dependence on the probe geometry and the velocity. With macroscopic probes, we observe that, for 3% agarose, the shear stress weakly increases with decreasing probe diameter and increasing probe velocity. These measurements indicate that agarose mildly deviates from an ideal continuous medium, but the magnitudes of these trends are small and do not affect our force calculation significantly.

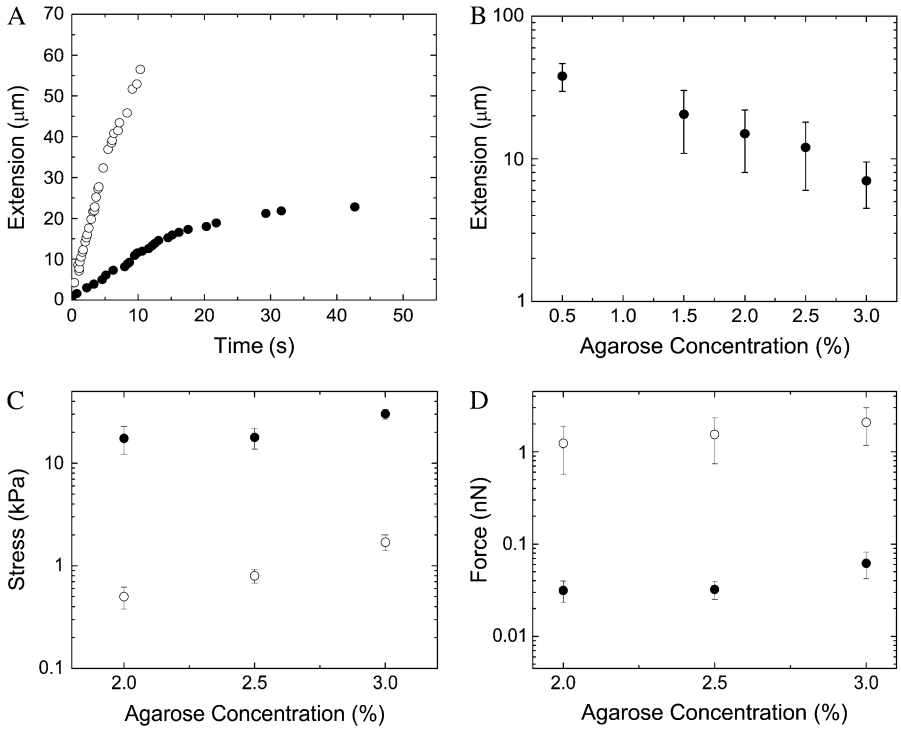

FIGURE 3 (*A*) Graph shows typical extension for a sperm cell in sea water (*open circle*), and a cell in 2% agarose (*solid circle*). Note the cell in agarose stalls at 20 μm. (*B*) Stall lengths of the acrosome bundle decrease as agarose concentration increases. (*C*) Agarose characterization results for a stainless steel needle of $R_{rod} = 0.54$ mm. Stress versus agarose concentrations. Solid circles are crack-opening stress values, and open circles represent the shear stress. (*D*) Shear (*open circles*) and crack opening (*solid circles*) forces exerted on acrosome bundle. Total acrosome force at the moment of stalling is found by summing both crack opening and shear drag forces, $F_s = F_{crack} + F_{drag}$. We have consistent values of the total stalling force at all concentrations of agarose, with an average $F_s \sim 1.9$ nN.

As an independent means to verifying these measurements, we used a solution of methyl cellulose (MC) and ASW to mechanically slow down the extension rate of the acrosome bundle. Unlike the experiments with agarose, the acrosome bundle is able to extend to its full length with a finite final velocity. For the acrosome bundle to extend in a viscous medium at a finite velocity, the force generated by the acrosome reaction must at all times exceed the opposing viscous drag, and thus the maximum drag force exerted by the environment yields a lower bound of the acrosome reaction force. For a viscoelastic fluid, the drag force F_V can be found by using the Stokes equation for a cylinder (18) only in the limiting case of viscous regime with Deborah number $(De) \ll 1$,

$$F_V \sim \frac{2\pi\mu_m x v}{\ln(x/2R_a) - 0.2}, \quad (2)$$

where μ_m is the viscosity of the MC solution, x is the length of the extended bundle, and v is the velocity of the extension at the length x. A MC solution of 4% (w/v) or lower exhibits a Newtonian viscous liquidlike behavior with $De \ll 1$, while one 5% or above behaves more like an elastic solid. We obtain a maximum lower bound force using the viscosity from the 4% MC solution. For a strain rate of 0.2 s^{-1}, which is the characteristic strain rate for the extending acrosome bundle in the 4% MC solution, the viscosity μ_m is measured to be $\sim$5 Pa · s. Using Eq. 2, the average force values at 4% MC is calculated to be $F_{low} \sim 260$ pN, and provides a lower-bound estimate for the force of the acrosome reaction. This is approximately a seventh of the upper-bound force obtained from stalling experiments, further substantiating the validity of our force estimates.

To determine whether the mechanical force of the acrosome reaction is sufficient to puncture an egg surface, we measure the force required to puncture the vitelline layer of the *Limulus* egg (diameter $\sim$2 mm) using a 100-μm diameter platinum wire to push against the egg (Fig. 2 *D*). The puncturing pressure is calculated as $P_F = F_{max}/\pi R_{rod}^2$ and the average value from eight different eggs is 0.45 ± 0.06 MPa. Based on our stalling force measurements, $F_s \sim 1.9$ nN, the imposed pressure on the egg by the tip of the acrosome bundle is $\sim$1.56 MPa. Thus, the coiled actin bundle generates approximately three times the stress necessary to mechanically puncture the egg vitelline layer. In terms of the stall force, we can also estimate the amount of energy released during the reaction. Since the stall force is the maximum force the acrosome reaction can generate, the total energy dissipated over the average stalled length of $l \sim 7$ μm at 3% agarose is calculated to be, at most, $W = \tau\pi R l^2 \sim 1.58 \times 10^{-14}$ J. For comparison, the stored elastic energy of the 7-μm section of the bundle is 3.5×10^{-14} J, based on our earlier measurements of the twist strain and the twisting stiffness of the bundle (12,14). Thus the stored elastic energy associated with the overtwist of the actin filaments is fully capable of providing all the energy required to power the extension and provide a force to penetrate the vitelline layer. To compare with other modalities of actin-based cell motility, it is useful to view the dynamics of this spring in terms of a specific power. The entire bundle consists of roughly 1.1 million subunits of the actin-scruin-calmodulin complex and its total mass is 3.1×10^{-16} kg. Using a typical velocity of 10 μm/s and a stalling force of 1.9 nN yields a value of 65 W/kg for the specific power of the actin spring. Recent measurements

report the force generated by the actin polymerization motor to be ~2 nN per μm of the margin of the leading edge of a lamellipodium (19). For a typical leading edge of 50 μm $\times$ 0.176 μm $\times$ 5 μm volume, the mass of actin monomers participating in the polymerization motor is estimated to be 1.8×10^{-15} kg. With a velocity for filamentous actin of 0.26 μm/s, we obtain a specific power of 13 W/kg for the polymerization motor. At a cellular level, the simple mechanochemical spring represents a powerful engine and its specific power is almost five times larger than that of a lamellipodium.

For the sperm cells of marine invertebrates such as the horseshoe crab, the vitelline layer of the egg presents a formidable physical barrier to fertilization. The solution to this biological problem lies in a chemically triggered version of a simple engineering device—a spring. We have quantified the ability of this actin spring to store and release elastic energy, and to mechanically produce force and motion. From these purely conformational changes, the sperm cell is able to puncture the protective layers of the egg and achieve fertilization.

We thank Jorge Ferrer for help with the optical setup.

This work was supported by a National Science Foundation Graduate Research fellowship and Basic Research Fund of the Korea Institute of Machinery and Materials to J.H.S., a Lemelson Foundation Fellowship to R.R.B., the MIT/NIGMS Biotechnology Training Program to R.R.B., the Center for Biomedical Engineering at MIT to P.M., and the National Institutes of Health (GM52703) to P.M.

REFERENCES

1. Pollard, T. D. 1986. Assembly and dynamics of the actin filament system in nonmuscle cells. *J. Cell. Biochem.* 31:87–91.
2. Warrick, H., and J. Spudich. 1987. Myosin structure and function in cell motility. *Annu. Rev. Cell Biol.* 3:379–421.
3. Mahadevan, L., and P. Matsudaira. 2000. Motility powered by supramolecular springs and ratchets. *Science*. 288:95–100.
4. Finer, J., R. Simmons, and J. Spudich. 1994. Single myosin molecule mechanics: picoNewton forces and nanometer steps. *Nature*. 368:113–119.
5. Dogterom, M., and B. Yurke. 1997. Measurement of the force-velocity relation for growing microtubules. *Science*. 278:856–860.
6. Linke, W. A., V. I. Popov, and G. H. Pollark. 1994. Passive and active tension in single cardiac myofibrils. *Biophys. J.* 67:782–792.
7. Ponti, A., M. Machacek, S. L. Gupton, C. M. Waterman-Storer, and G. Danuser. 2004. Two distinct actin networks drive the protrusion of migrating cells. *Science*. 305:1782–1786.
8. Marcy, Y., J. Prost, M. Carlier, and C. Sykes. 2004. Forces generated during actin-based propulsion: a direct measurement by micromanipulation. *Proc. Natl. Acad. Sci. USA*. 101:5992–5997.
9. Brown, G. G., and W. J. Humphreys. 1971. Sperm-egg interactions of *Limulus polyphemus* with scanning electron microscopy. *J. Cell Biol.* 51:904–907.
10. Tilney, L. 1975. Actin filaments in the acrosome reaction of *Limulus* sperm. *J. Cell Biol.* 64:289–310.
11. Sanders, M., M. J. Way, J. Sakai, and P. Matsudaira. 1996. Characterization of the actin crosslinking properties of the scruin-CaM complex from the acrosomal process of the *Limulus* sperm. *J. Biol. Chem.* 271:2651–2657.
12. Shin, J. H., L. Mahadevan, G. S. Waller, K. Langsetmo, and P. Matsudaira. 2003. Stored elastic energy powers the 60-μm extension of the *Limulus* polyphemus sperm actin bundle. *J. Cell Biol.* 162:1183–1188.
13. DeRosier, D., L. Tilney, and P. Flicker. 1980. A change in the twist of the actin-containing filaments occurs during the extension of the acrosomal process in *Limulus* sperm. *J. Mol. Biol.* 137:375–389.
14. Shin, J., L. Mahadevan, P. T. So, and P. Matsudaira. 2004. Bending stiffness of a crystalline actin bundle. *J. Mol. Biol.* 337:255–261.
15. Schmid, M., M. Sherman, P. Matsudaira, and W. Chiu. 2004. Structure of the acrosomal bundle. *Nature*. 431:104–107.
16. Kusukawa, N., M. V. Ostrovsky, and M. M. Garner. 1991. Effect of gelation conditions on the gel structure and resolving power of agarose-based DNA sequencing gels. *Electrophoresis*. 20:1455–1461.
17. Fatin-Rouge, N., K. Starchev, and J. Buffle. 2004. Size effects on diffusion processes within agarose gels. *Biophys. J.* 86:2710–2719.
18. Tirado, M. M., and J. Garcia de la Torre. 1979. Translational friction coefficients of rigid symmetric top macromolecules: application to circular cylinders. *J. Chem. Phys.* 71:2581–2587.
19. Abraham, V. C., V. Krishnamurthi, D. L. Taylor, and F. Lanni. 1999. The actin-based nanomachine at the leading edge of migrating cells. *Biophys. J.* 77:1721–1732.